



Activity Stabilization in a Population Model of Working Memory by Sinusoidal and Noisy Inputs

Nikita Novikov^{1*}, Denis Zakharov^{1*}, Victoria Moiseeva¹ and Boris Gutkin^{1,2*}

¹ Centre for Cognition and Decision Making, HSE University, Moscow, Russia, ² Group for Neural Theory, LNC2 INSERM U960, Département d'Études Cognitives, École Normale Supérieure, PSL Research Université, Paris, France

OPEN ACCESS

Edited by:

Emmanuel Procyk,
Institut National de la Santé et de la
Recherche Médicale (INSERM),
France

Reviewed by:

Axel Hutt,
Inria Nancy – Grand-Est Research
Centre, France
Alex Roxin,
Centre de Recerca Matemàtica, Spain

*Correspondence:

Nikita Novikov
nikknovikov@gmail.com
Denis Zakharov
dgzakharov@hse.ru;
dzakh76@gmail.com
Boris Gutkin
boris.gutkin@ens.fr

Received: 30 December 2020

Accepted: 19 March 2021

Published: 21 April 2021

Citation:

Novikov N, Zakharov D,
Moiseeva V and Gutkin B (2021)
Activity Stabilization in a Population
Model of Working Memory by
Sinusoidal and Noisy Inputs.
Front. Neural Circuits 15:647944.
doi: 10.3389/fncir.2021.647944

According to mechanistic theories of working memory (WM), information is retained as stimulus-dependent persistent spiking activity of cortical neural networks. Yet, how this activity is related to changes in the oscillatory profile observed during WM tasks remains a largely open issue. We explore joint effects of input gamma-band oscillations and noise on the dynamics of several firing rate models of WM. The considered models have a metastable active regime, i.e., they demonstrate long-lasting transient post-stimulus firing rate elevation. We start from a single excitatory-inhibitory circuit and demonstrate that either gamma-band or noise input could stabilize the active regime, thus supporting WM retention. We then consider a system of two circuits with excitatory intercoupling. We find that fast coupling allows for better stabilization by common noise compared to independent noise and stronger amplification of this effect by in-phase gamma inputs compared to anti-phase inputs. Finally, we consider a multi-circuit system comprised of two clusters, each containing a group of circuits receiving a common noise input and a group of circuits receiving independent noise. Each cluster is associated with its own local gamma generator, so all its circuits receive gamma-band input in the same phase. We find that gamma-band input differentially stabilizes the activity of the “common-noise” groups compared to the “independent-noise” groups. If the inter-cluster connections are fast, this effect is more pronounced when the gamma-band input is delivered to the clusters in the same phase rather than in the anti-phase. Assuming that the common noise comes from a large-scale distributed WM representation, our results demonstrate that local gamma oscillations can stabilize the activity of the corresponding parts of this representation, with stronger effect for fast long-range connections and synchronized gamma oscillations.

Keywords: gamma oscillations, noise, in-phase oscillations, anti-phase oscillations, AMPA, NMDA, working memory

INTRODUCTION

The concept of working memory (WM) characterizes the ability of the brain to retain in an active form certain information that is relevant to a current task, but is not perceived at the particular moment by sensory systems (Baddeley, 2003). One of the main mechanisms supposedly underlying WM is self-sustained activity of neural populations (Goldman-Rakic, 1995; Compte, 2006), which

can be turned on or off in a short period of time (about 100 ms) and continue for a time interval of up to tens of seconds (Wang, 2001). Cells whose activity is maintained at an elevated level during the retention of information in WM have been found in various parts of the brain, primarily in the prefrontal cortex (Fuster and Alexander, 1971; Funahashi et al., 1989; Miller et al., 1996; Chafee and Goldman-Rakic, 1998; Constantinidis and Goldman-Rakic, 2002).

The process of retaining information in WM is also associated with changes in the collective rhythmic activity of brain networks (which are neuronal oscillations) in various frequency bands (Sauseng et al., 2009; Siegel et al., 2009; Haegens et al., 2010; Liebe et al., 2012; Kornblith et al., 2016; Lundqvist et al., 2016, 2018; Wimmer et al., 2016). Among these changes, increase of the gamma-band activity is of special interest. Gamma activity usually reflects activation of neural populations and coincides with episodes of firing rate elevation. In WM tasks, gamma activity increases most strongly during presentation of stimuli (Kornblith et al., 2016; Lundqvist et al., 2016; Wimmer et al., 2016), but in the delay period (i.e., in the time period after stimulus termination and before an instruction to make a response) it is still higher than in the baseline (Lutzenberger et al., 2002; Kaiser et al., 2003; Jokisch and Jensen, 2007; Haegens et al., 2010; Palva et al., 2011; Kornblith et al., 2016; Lundqvist et al., 2016; Wimmer et al., 2016). We note that during this delay period, the subject has to withhold the response, yet needs to retain “on-line” information necessary to generate the appropriate response. The delay-period gamma activity presumably reflects activation of the neural populations that represent the WM content (Roux and Uhlhaas, 2014). This is supported by the findings that the delay-period gamma activity is higher than in the passive observation task (Wimmer et al., 2016), increases with WM load (Howard et al., 2003; van Vugt et al., 2010; Kornblith et al., 2016; Lundqvist et al., 2016) and only in the task-relevant regions (Kaiser et al., 2003; Jokisch and Jensen, 2007) or at those cortical sites that contain neurons selective to the WM content (Kornblith et al., 2016; Lundqvist et al., 2016).

Recently, the delay-period gamma oscillations were more directly linked to activation of WM representations. It was demonstrated that gamma activity is irregular at the single-trial level, and the episodes of increased gamma power (“gamma-bursts”) are associated with elevated firing rates and increased amount of information about the WM content that could be decoded from spiking activity (Lundqvist et al., 2016, 2018; Bastos et al., 2018). It is not fully clear, however, whether the gamma power increase plays a functional role in WM retention or is it merely a consequence of transient firing rate increase during spontaneous reactivations of WM representations.

Besides the gamma power increase, an increase in gamma-band coherence between different cortical sites during the delay period was reported (Lutzenberger et al., 2002; Kaiser et al., 2003; Palva et al., 2010; Kornblith et al., 2016). Furthermore, it was shown that transcranial gamma-band electrical stimulation of two distant sites could improve performance in a WM task (Tseng et al., 2016). Interestingly, the improvement was observed only under anti-phase (but not under in-phase) stimulation.

This result suggests that gamma-band coherence presumably plays a functional role in WM retention, and is not merely an epiphenomenon.

Nowadays, a number of computational WM models exist. Most of them are based on multistable neural networks. In the simplest case, a system has two stable states, one of which (with low firing rates) corresponds to the background regime, and the other one (with higher firing rates) relates to the active regime, in which an object is retained in WM. Transition from the background to the active state occurs under the action of a short excitatory pulse that mimics the arrival of a to-be-memorized stimulus. As an alternative, there are models, in which the active retention regime is metastable, and the system slowly returns to the background state after a stimulus presentation (Lim and Goldman, 2013). In many WM models, the self-sustained post-stimulus firing rate elevation is provided by reverberation of excitation in the network due to synaptic interactions (Amit and Brunel, 1997; Brunel and Wang, 2001). In addition, there are models in which post-stimulus enhancement of synaptic connections due to short-term plasticity plays a significant role (Mongillo et al., 2008, 2012; Hansel and Mato, 2013).

Many theoretical papers, following Amit and Brunel (1997), described WM models with asynchronous spiking activity. It was shown that if a model contains only fast excitation, then even slight synchronization returns it to the background state (Gutkin et al., 2001; Laing and Chow, 2001; Compte, 2006). However, generation of oscillations (i.e., synchronization) in a WM model is possible in the presence of slow NMDA receptors (Tegnér et al., 2002) or in the case of modular structure of the system (Lundqvist et al., 2010, 2011). Besides investigating the mechanisms of oscillations’ appearance in WM models (Tegnér et al., 2002; Roxin and Compte, 2016), several theoretical studies explore possible functional roles of oscillations in WM (Lisman and Idiart, 1995; Ardid et al., 2010; Lundqvist et al., 2010, 2011; Kopell et al., 2011; Chik, 2013; Dipoppa and Gutkin, 2013; Pina et al., 2018; Schmidt et al., 2018; Sherfey et al., 2020). The methodology, however, differs substantially between these studies, and a unified theoretical framework in this field is still lacking.

We follow a paradigm used in Dipoppa and Gutkin (2013); Schmidt et al. (2018), in which a WM system is resonant and receives an external oscillatory input that controls its behavior. Schmidt et al. (2018) showed that gamma-band input could stabilize WM retention even if the active regime is initially metastable (which means that the firing rate increases after stimulus presentation, but then slowly returns to the background level in the absence of input oscillations). In the present study, we make a step further and consider systems with metastable active regime that are comprised of several excitatory-inhibitory circuits coupled by symmetrical excitatory connections and receiving the same stimulus-related signal (such systems could serve as models of a distributed representation of an object in WM). We explore stabilization of the metastable active regime by external gamma-band and white-noise inputs, both of which are assumed to come from neural populations not explicitly included into the model.

We assume that the gamma-band inputs are generated locally (and thus could have different phases for different

circuits), and that the noise inputs originate from distributed networks (that could jointly participate in WM retention, thus producing correlated activity). The model parameters in the focus of our research are the following: (1) in-phase or anti-phase character of the gamma inputs to the circuits, (2) commonality or independence of the noise inputs to the circuits, (3) NMDA:AMPA ratio of inter-circuit connections. By varying these parameters, we aim to understand whether gamma-band oscillations are able to preferentially stabilize the active regime in those circuits that participate in collective WM-related activity (and thus receive a common noise input rather than independent inputs). Another goal of our study is to explore whether synchronization of gamma generators (leading to in-phase gamma inputs to different circuits) affects the ability of the gamma input to stabilize WM retention, depending on whether the inter-circuit connection in the system are fast or slow.

The paper is organized as follows. We start from a single-circuit model and demonstrate that the active regime could be stabilized by gamma-band or white-noise input. Next, we explore joint stabilizing effect of gamma-band and white-noise inputs in a system of two circuits with mutual excitation. We vary the NMDA:AMPA ratio of the inter-circuit connections and parameters of the inputs (including phase difference between the gamma inputs to the circuits and commonality/independence of the noise inputs); for each parameter combination we evaluate the effectiveness of stabilization. Finally, we consider a multi-circuit system comprised of two local clusters, with all the circuits in a cluster receiving the same gamma input. Each cluster, in turn, contains two circuit groups: the circuits from the first groups receive a common noise input and the circuits from the second groups – independent noise inputs. We explored the stabilizing effect of gamma input on each circuit group, depending on whether it is delivered to the clusters in the same phase or in the anti-phase, conditioned on the type (slow/fast) of the inter-cluster connections.

MATERIALS AND METHODS

Model Description

In this article, we consider firing rate models of WM that consist of one, two, or many circuits each containing interacting excitatory and inhibitory neural populations (**Figure 1**). These circuits serve as representations of various parts or features of WM content and are linked by symmetrical excitatory connections. Each circuit receives an external input consisting of several components: (1) tonic (constant) input, (2) stimulus-related input, (3) zero-mean sinusoidal oscillatory input, and (4) white noise. The stimulus-related input is implemented as a rectangular pulse whose amplitude and duration are the same for all circuits in the model. The stimulus input is projected 80% to the excitatory population of a circuit and 20% to the inhibitory population. The oscillatory input impinges only on the excitatory populations of circuits and represents a modulatory

signal from the outside of the modeled WM network. White noise mimics the input produced by activity of a larger network into which our model is embedded, but which was not modeled explicitly. We explore different cases, in which the circuits receive in-phase or anti-phase oscillatory inputs, as well as identical or independent noisy inputs.

The state of circuit populations is described by the following dynamical variables: (1) firing rates, (2) mean input currents (AMPA, NMDA, and GABAA), and (3) population variances of the input currents (AMPA and GABAA). We further argue that if the mean values of the AMPA and NMDA currents are of the same order of magnitude, the NMDA current variance has to be much smaller than the AMPA variance, since the NMDA time constant is much larger than the AMPA time constant. Hence, we set the NMDA current variance to zero. Thus, our model of interacting circuits is described by the following equations:

$$\begin{cases} \tau_{ra} \frac{dr_a^p}{dt} = -r_a^p + F_{ra}(\mu_a^p, \sigma_{a,AMPA}^p, \sigma_{a,GABAA}^p) \\ \mu_a^p = \sum_S \mu_{a,S}^p, \quad S = AMPA, NMDA, GABAA \\ \tau_S \cdot \frac{d\mu_{a,S}^p}{dt} = -\mu_{a,S}^p + \tilde{\mu}_{a,S}^{p,rec} + \tilde{\mu}_{a,S}^{p,cc} + \tilde{\mu}_{a,S}^{p,ext} \\ \frac{\tau_S}{2} \cdot \frac{d(\sigma_{a,S}^p)^2}{dt} = -(\sigma_{a,S}^p)^2 + (\tilde{\sigma}_{a,S}^{p,rec})^2 + (\tilde{\sigma}_{a,S}^{p,cc})^2 + (\tilde{\sigma}_{a,S}^{p,ext})^2 \end{cases}$$

where, the lower index a denotes a population type (e , excitatory; i , inhibitory), the upper index p denotes a circuit number. The variable r_a^p is the firing rate; μ_a^p is the total mean input current, $\mu_{a,S}^p$ is the mean input current via the synapses of the type S (S denotes AMPA, NMDA, or GABAA); $(\sigma_{a,S}^p)^2$ is a population variance of the input current via the synapses of the type S ; τ_{ra} is the time constant that governs the firing rate dynamics, τ_S is the synaptic time constant for the synapses of the type S ; $\tilde{\mu}_{a,S}^{p,rec}$, $(\tilde{\sigma}_{a,S}^{p,rec})^2$ are the population mean and variance of the recurrent (intra-circuit) inputs; $\tilde{\mu}_{a,S}^{p,cc}$, $(\tilde{\sigma}_{a,S}^{p,cc})^2$ are the population mean and variance of the input from other modeled circuits; $\tilde{\mu}_{a,S}^{p,ext}$ and $(\tilde{\sigma}_{a,S}^{p,ext})^2$ are the population mean and variance of the external inputs; F_{ra} are the gain (transfer) functions. Note that the time constant for the population variance of each current is twice smaller than the time constant for the population mean of the same current (due to the properties of linear first-order stochastic ODE's; (see Renart et al., 2007) for an example of a model with dynamical mean and variance of the input current). Within-circuit excitatory-to-excitatory connections demonstrate short-term plasticity (Tsodyks and Markram, 1997), see the full description in the **Supplementary Material**.

We also need to define the gain functions for the neural populations. Instead of defining these gain functions F_{re} and F_{ri} *a priori*, we calculate them following an approach similar to the one previously used in Schaffer et al. (2013) and Augustin et al. (2017) that allows to match low-dimensional models with spiking networks, making them more biologically plausible. According to this approach, the gain functions were

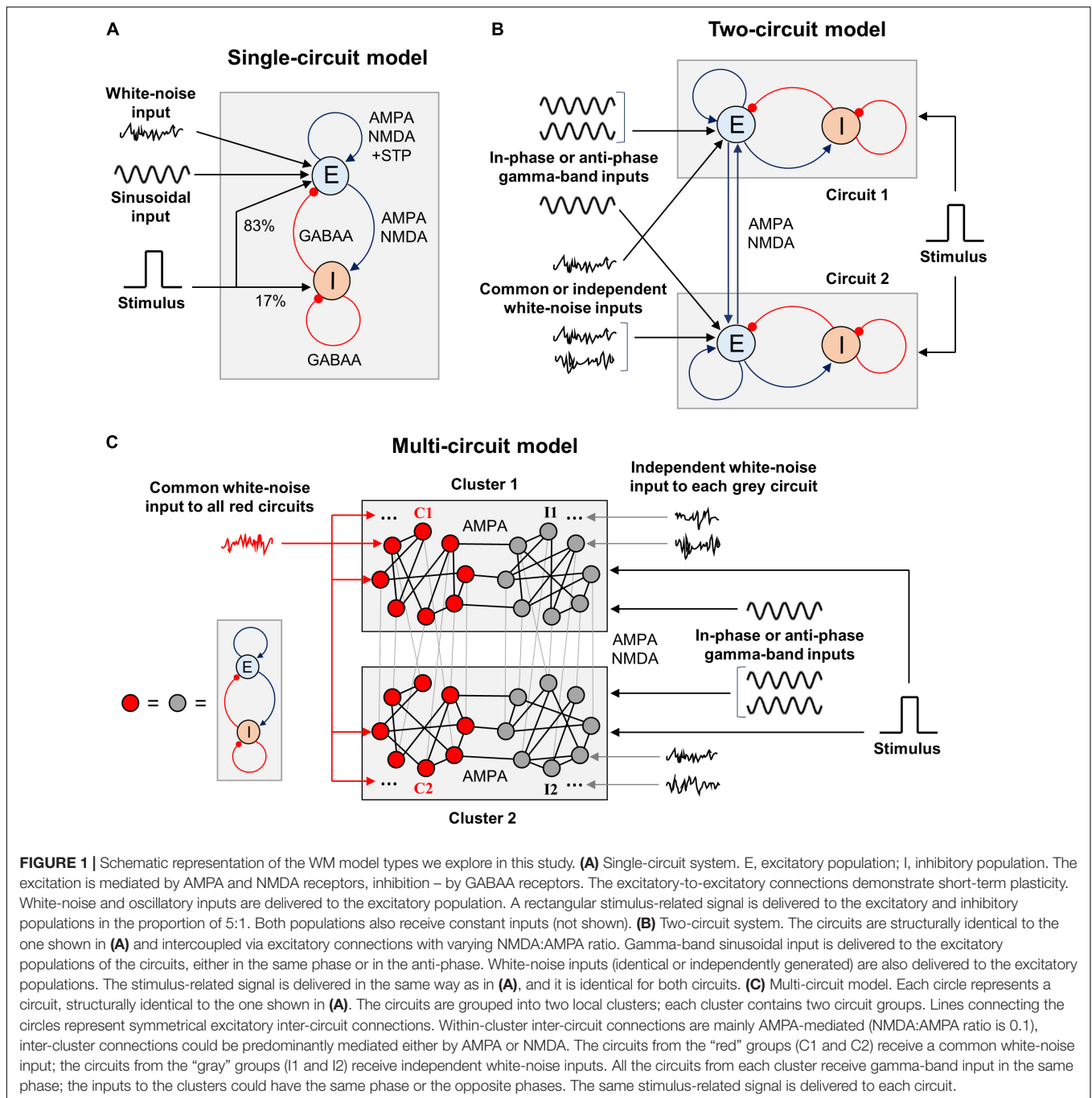
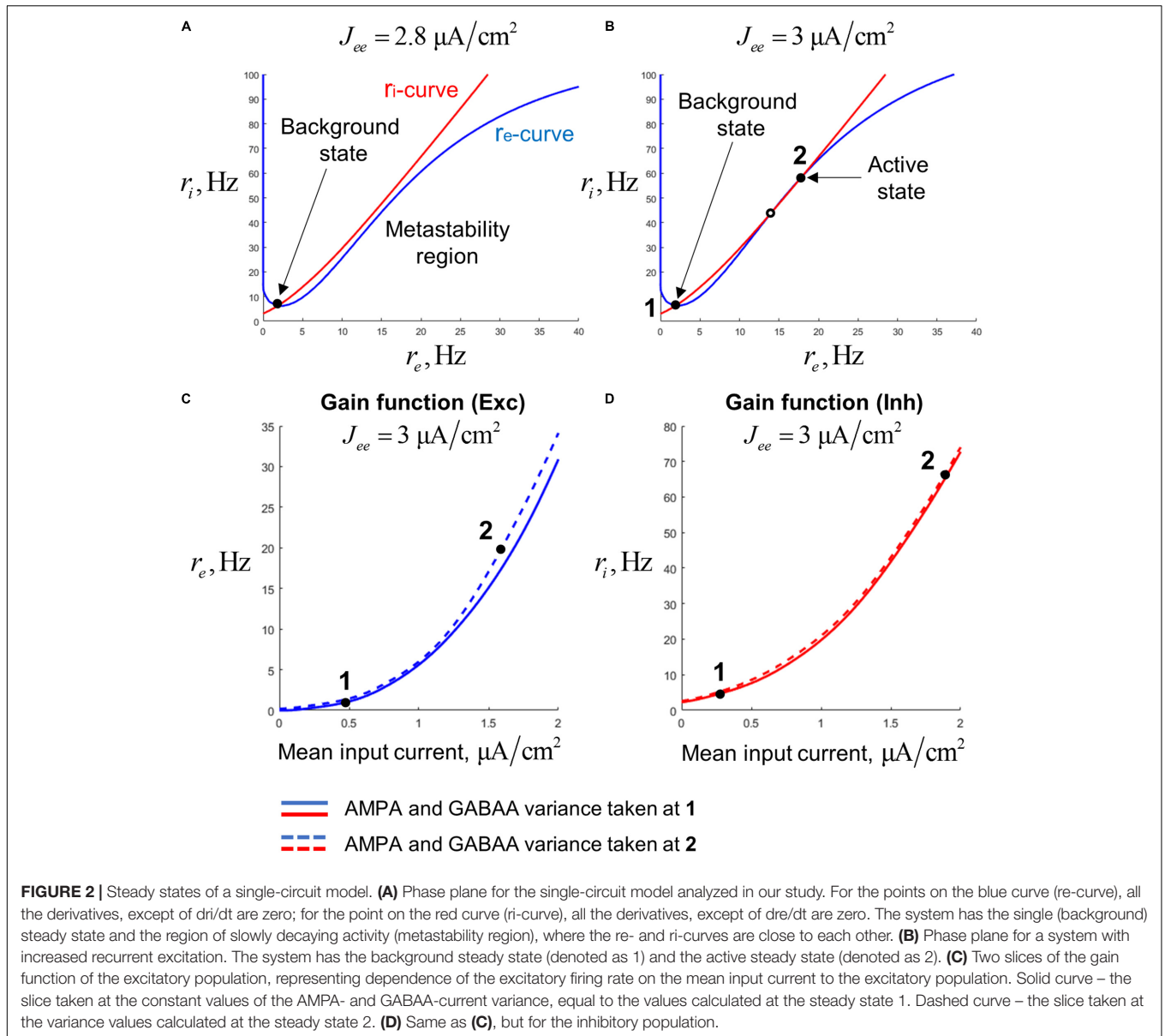


FIGURE 1 | Schematic representation of the WM model types we explore in this study. **(A)** Single-circuit system. E, excitatory population; I, inhibitory population. The excitation is mediated by AMPA and NMDA receptors, inhibition – by GABA receptors. The excitatory-to-excitatory connections demonstrate short-term plasticity. White-noise and oscillatory inputs are delivered to the excitatory population. A rectangular stimulus-related signal is delivered to the excitatory and inhibitory populations in the proportion of 5:1. Both populations also receive constant inputs (not shown). **(B)** Two-circuit system. The circuits are structurally identical to the one shown in **(A)** and intercoupled via excitatory connections with varying NMDA:AMPA ratio. Gamma-band sinusoidal input is delivered to the excitatory populations of the circuits, either in the same phase or in the anti-phase. White-noise inputs (identical or independently generated) are also delivered to the excitatory populations. The stimulus-related signal is delivered in the same way as in **(A)**, and it is identical for both circuits. **(C)** Multi-circuit model. Each circle represents a circuit, structurally identical to the one shown in **(A)**. The circuits are grouped into two local clusters; each cluster contains two circuit groups. Lines connecting the circles represent symmetrical excitatory inter-circuit connections. Within-cluster inter-circuit connections are mainly AMPA-mediated (NMDA:AMPA ratio is 0.1), inter-cluster connections could be predominantly mediated either by AMPA or NMDA. The circuits from the “red” groups (C1 and C2) receive a common white-noise input; the circuits from the “gray” groups (I1 and I2) receive independent white-noise inputs. All the circuits from each cluster receive gamma-band input in the same phase; the inputs to the clusters could have the same phase or the opposite phases. The same stimulus-related signal is delivered to each circuit.

pre-calculated on a cubic grid (with the coordinates: total mean current, AMPA current std., and GABA current std.) by numerical simulations of leaky integrate-and-fire (LIF) neurons having typical properties of the regular-spiking (pyramidal) neurons and the fast-spiking interneurons of the cortex. For an arbitrary point, the value of a gain function was obtained by interpolation between the pre-calculated values at the closest grid nodes. To show the shape of the gain functions, in **Figures 2C,D** we present their projections to the plane of mean firing rate and total mean input current. The projections

were made for two different combinations of AMPA and GABA current std. that correspond to the background and active states of the bistable single-circuit system (these states are depicted in **Figure 2A**; see the next section for details). Since our model is tuned to operate in a subthreshold regime [which is typical for cortical neurons; (Compte et al., 2003; Wang, 2010)], the aforementioned plots have an exponential-like, concave shape.

The full system of model equations and its detailed description are given in the **Supplementary Material**.



Model Parameters

Single Circuit

We set the parameters of a circuit (**Figure 1A**) in such way that: (1) it has a stable background steady state with a low level of activity, (2) it responds to a stimulus by prolonged activity increase with subsequent return to the vicinity of the background state, and (3) it has gamma-band resonance during the post-stimulus increased activity. We refer to the increased post-stimulus activity as metastable active regime and refer to a system with such regime as metastable system.

To obtain the required behavior of the circuit (metastability and gamma-band resonance), we set the parameters in the following way. We start by pre-selecting parameters that provide bistability in a circuit. In this case, there are three equilibria

in the phase space: two stable ones (corresponding to the background and active states) and a saddle (**Figure 2B**). We tuned the parameters in such way that the second (active) equilibrium has a pair of complex-conjugate eigenvalues with a small negative real part and an imaginary part corresponding to the gamma band. An orbit of such a system, when starting near the active steady state, shows slowly decaying gamma-band oscillations returning back to the active state (an example is presented in **Supplementary Figure 1B**). Then, we decreased the weight of the excitatory-to-excitatory synaptic connections, until the upper equilibrium disappears through a fold bifurcation (see the phase plane with the single steady state in **Figure 2A**). In fact, the upper equilibrium leaves a “ghost” near which the dynamics are slow. Thus, the resulting

system is metastable, and the slow dynamics near the “ghost” corresponds to the metastable active regime. This regime inherits gamma-band resonance from the active steady state that existed in the bistable system before the bifurcation. An example orbit of the metastable system showing damped oscillations with subsequent decay to the background is presented in **Supplementary Figure 1A**.

Finally, we explored the ability of white-noise and sinusoidal inputs to stabilize the metastable active regime.

Two Circuits

We also considered a system of two identical interacting circuits (**Figure 1B**). In this case, we symmetrically connect the circuits using excitatory coupling between their excitatory populations. At the same time, to compensate this additional inter-circuit excitation, we decreased the background inputs to the excitatory populations. In this way, we keep the metastable behavior in each circuit and could study the influence of input oscillations and noise.

We varied NMDA:AMPA ratio for the inter-circuit connections and explored the ability of in-phase/anti-phase oscillatory inputs and common/independent white-noise inputs to stabilize the active regime. We used duration of increased post-stimulus activity as the measure of the active regime stability. The post-stimulus activity of a circuit was considered to be terminated when the time-course of its excitatory population firing rate smoothed with the 100 ms time window fell below the level of 3 Hz.

Multiple Circuits

Finally, we considered a multi-circuit system schematically presented in **Figure 1C**. Each circuit is represented by a (red or black) circle. Links between the circles correspond to mutual excitatory connections between the circuits. In the system considered, there were two circuit clusters that mimic two spatially separated local networks. All circuits in each cluster receive input oscillations of the same phase, whereas the circuits in different clusters may receive either in-phase or anti-phase oscillations.

Each cluster contains two groups of circuits. Circuits from the first groups C1, C2 (red-colored circuits in both clusters in **Figure 1C**) receive a common noise input. Circuits from the second groups I1, I2 (gray circuits in **Figure 1C**) receive independent noise inputs.

Each group in our model is a random graph with eight nodes (circuits) having the constant in-degree of three; two groups within the same cluster (C1–I1 and C2–I2) are connected by three randomly assigned links; corresponding groups in different clusters (C1–C2 and I1–I2) are connected by eight randomly assigned links (with one link per each node); non-corresponding groups in different clusters (C1–I2 and C2–I1) are not connected. All links between circuits are bi-directional.

We considered two multi-circuit models: one with the fast inter-cluster connections (90% AMPA and 10% NMDA), and the other one with slow inter-cluster connections (100% NMDA). All other parameters were identical. We simulated

both models in several regimes: (1) no oscillatory input, (2) only one cluster receives oscillatory input, (3) the clusters receive in-phase oscillations, (4) the clusters receive anti-phase oscillations. For each regime, we were interested in the average duration of post-stimulus activity of each circuit group (C1, I1, C2, and I2).

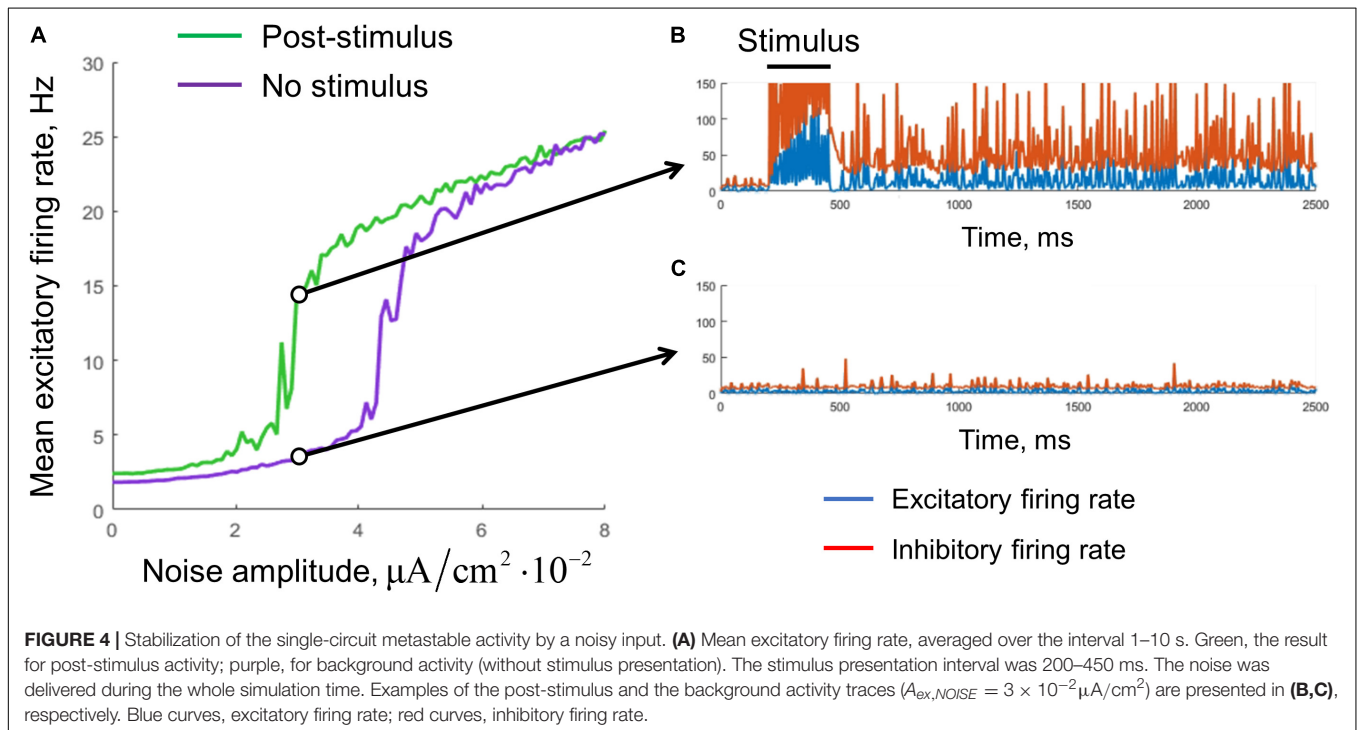
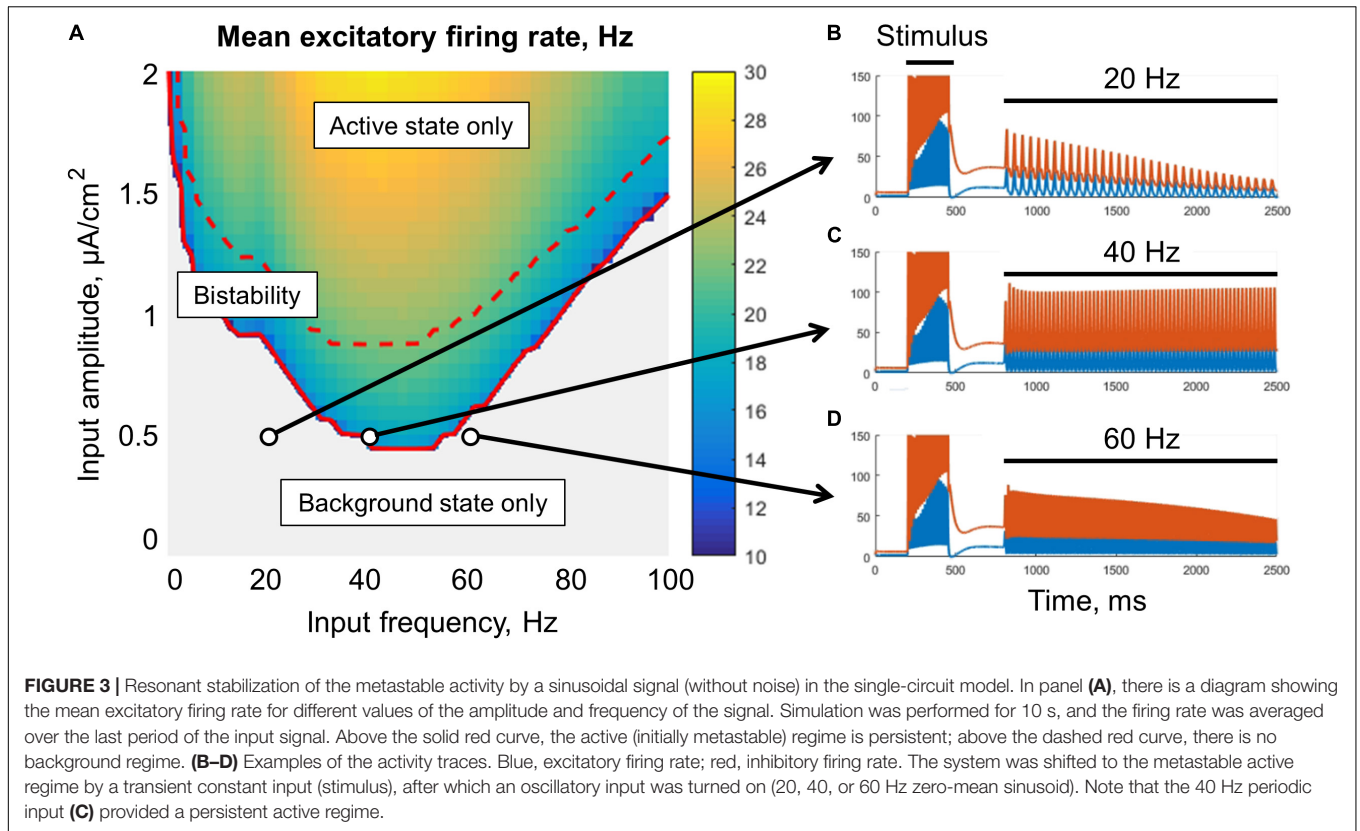
RESULTS

Activity of Single-Circuit Model

A single-circuit model consisting of an excitatory and an inhibitory population (**Figure 1A**) could be either bistable or monostable, depending on the strength of the self-excitation. For strong enough self-excitation, the model has three equilibria (**Figure 2B**): two stable steady states and a saddle. The stable equilibria correspond to two types of activity: the background (low-rate) and active (high-rate) regimes, while the saddle manifold separates their basins of attraction. For weaker self-excitation, the equilibria that correspond to the active state and the saddle disappear through the fold bifurcation, and a metastable active regime (with high firing rate) remains as a ghost of the active state (**Figure 2A**). In this case, the circuit could be excited from the background state by a stimulus and demonstrate relatively long transient high-firing-rate activity.

The metastable active regime can be stabilized (i.e., the decay of the post-stimulus activity could be slowed or prevented) either by an oscillatory signal (**Figure 3**), or by a noisy input (**Figure 4**). In the case of oscillatory input, there is a range of its amplitudes, for which the stabilization occurs only if the input frequency falls into the lower gamma band (middle part of **Figure 3A**). For lower amplitudes, the stabilization does not occur (gray region in **Figure 3A**). For higher amplitudes, the frequency range of stabilization expands to the high gamma and beta bands. If the input amplitude is too high (above the dashed red line in **Figure 3A**), the background regime disappears, i.e., the oscillations put the system into the active (high-firing-rate) regime even without stimulus presentation.

We found that noisy input is also able to stabilize the metastable state (**Figure 4**). The purple curve represents the mean firing rate observed in the absence of a stimulus, as a function of the noise standard deviation. The green curve represents the mean post-stimulus firing rate. At low intensity, the noise was unable to stabilize the active regime, while at high intensity, the noise put the system to the active regime even without stimulus presentation. Thus, an intermediate range of noise intensities is appropriate for WM functioning; it is seen in **Figure 4A** as the range in which the green line goes considerably above the purple line. For a value from this range, the persistent activity is initiated by a transient stimulus, and the WM trace is then kept “alive” by the noise input (**Figure 4B**). At the same time, the system stays in the background regime if the stimulus is not presented (**Figure 4C**).



Activity of Two-Circuit Model

In this section, we explore joint stabilizing effect of input noise and oscillations on the system of two circuits with mutual

excitatory connections (Figure 1B). We investigate different cases when circuits receive in-phase or anti-phase oscillations, as well as common or independent noise. The inter-circuit connections

contain both fast AMPA and slow NMDA components. We varied the proportion of the inter-circuit current that flows via NMDA receptors (which we denoted as k_{NMDA}^{cross}), while keeping the total inter-circuit connection strength at the constant level.

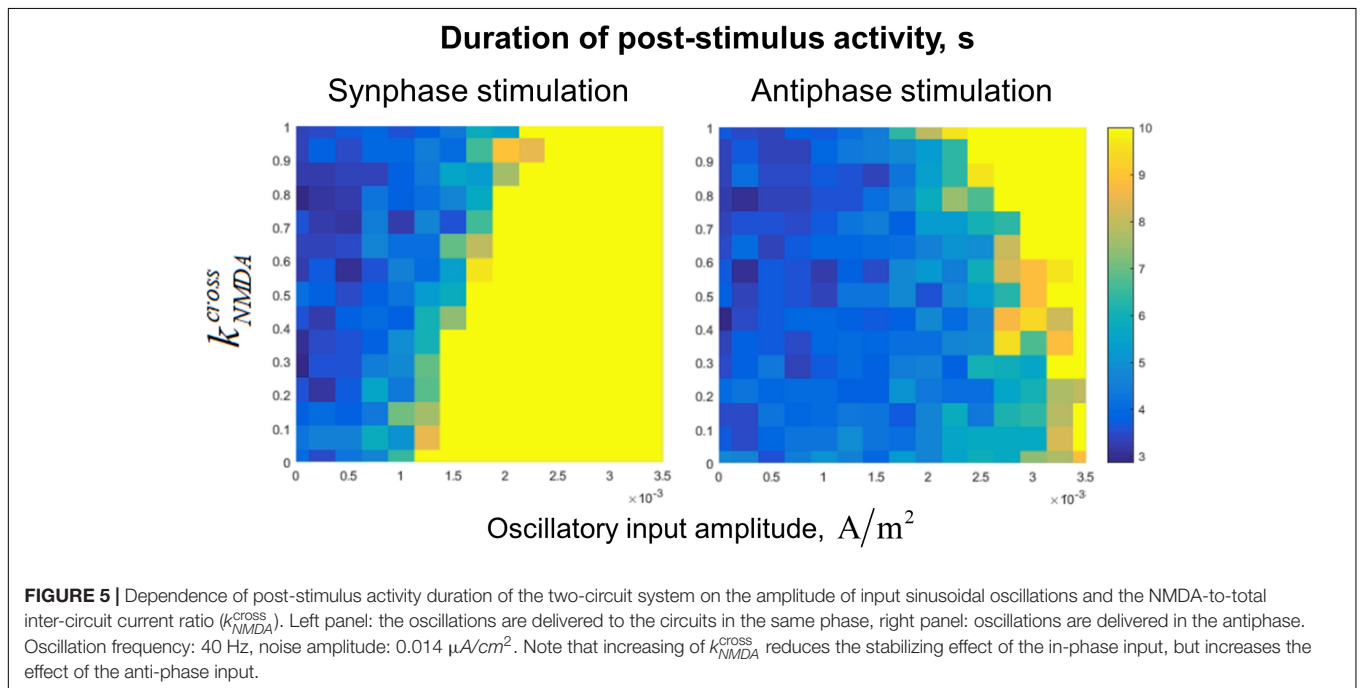
Dependence of the post-stimulus activity duration (which we use as the measure of the active regime stability) on k_{NMDA}^{cross} value and the amplitude of the input oscillations is presented in **Figure 5**. In the case of fast (AMPA) inter-circuit connections ($k_{NMDA}^{cross} = 0$), the in-phase oscillatory input to both circuits leads to stabilization of the active regime with high efficiency (**Figure 5**, lower part of the left panel). Anti-phase input oscillations in this case need to have a very high amplitude to stabilize the active regime (**Figure 5**, lower part of the right panel). With increasing k_{NMDA}^{cross} (i.e., the portion of the slow NMDA component of the inter-circuit current), effectiveness of the in-phase input deteriorates, while effectiveness of the anti-phase input increases (see the opposite trends in the left and right panels of **Figure 5**). For $k_{NMDA}^{cross} \cong 1$, both types of the input have approximately the same effect (**Figure 5**, upper parts of the panels).

In the presence of noise, our system generates irregular gamma-band quasi-oscillations. They act together with the external gamma-band input in stabilizing the active regime. The joint dependence of the post-stimulus activity duration on the input oscillations' amplitude and on the noise standard deviation is presented in **Figure 6**. In general, the activity duration increases when either the oscillations or the noise become stronger.

In the case of fast inter-circuit connections ($k_{NMDA}^{cross} = 0$, **Figures 6A,B**), common noise has stronger stabilizing

effect than independent noise (compare the left and middle panels of **Figures 6A,B**). This is true in the presence of either in-phase or anti-phase oscillations, but in the case of anti-phase oscillations, the stabilizing effect occurs at much higher amplitudes compared to in-phase oscillations (see different horizontal scales in **Figures 6A,B**). The yellow region in the right panels of **Figures 6A,B** contains the combinations of oscillations' amplitude and noise standard deviation, for which there is an evident difference in the post-stimulus activity duration between the common-noise and the independent-noise cases (within our simulation time). Importantly, for intermediate noise intensities, an evident difference is observed only if the oscillations are sufficiently strong (see the horizontal black lines in the right panels of **Figures 6A,B** cross the yellow region near the right parts of the diagrams). In other words, an external gamma-band input with an appropriate amplitude stabilizes the active regime (i.e., WM retention) only when the two circuits receive a common noise input (e.g., when they belong to the same distributed representation), but not when they receive independent noise inputs of the same strength (e.g., when they are parts of different representations).

In the case of slow inter-circuit connections ($k_{NMDA}^{cross} = 1$, **Figures 6C,D**), common noise has weaker stabilizing effect than independent noise (compare the left and middle panels of **Figures 6A,B**). This difference, however, is less pronounced than in the case of fast inter-circuit connections (compare the right panels of **Figures 6A–D**). Furthermore, in-phase and anti-phase gamma-band inputs have almost the same effect (compare **Figures 6C,D**, note that the horizontal scale



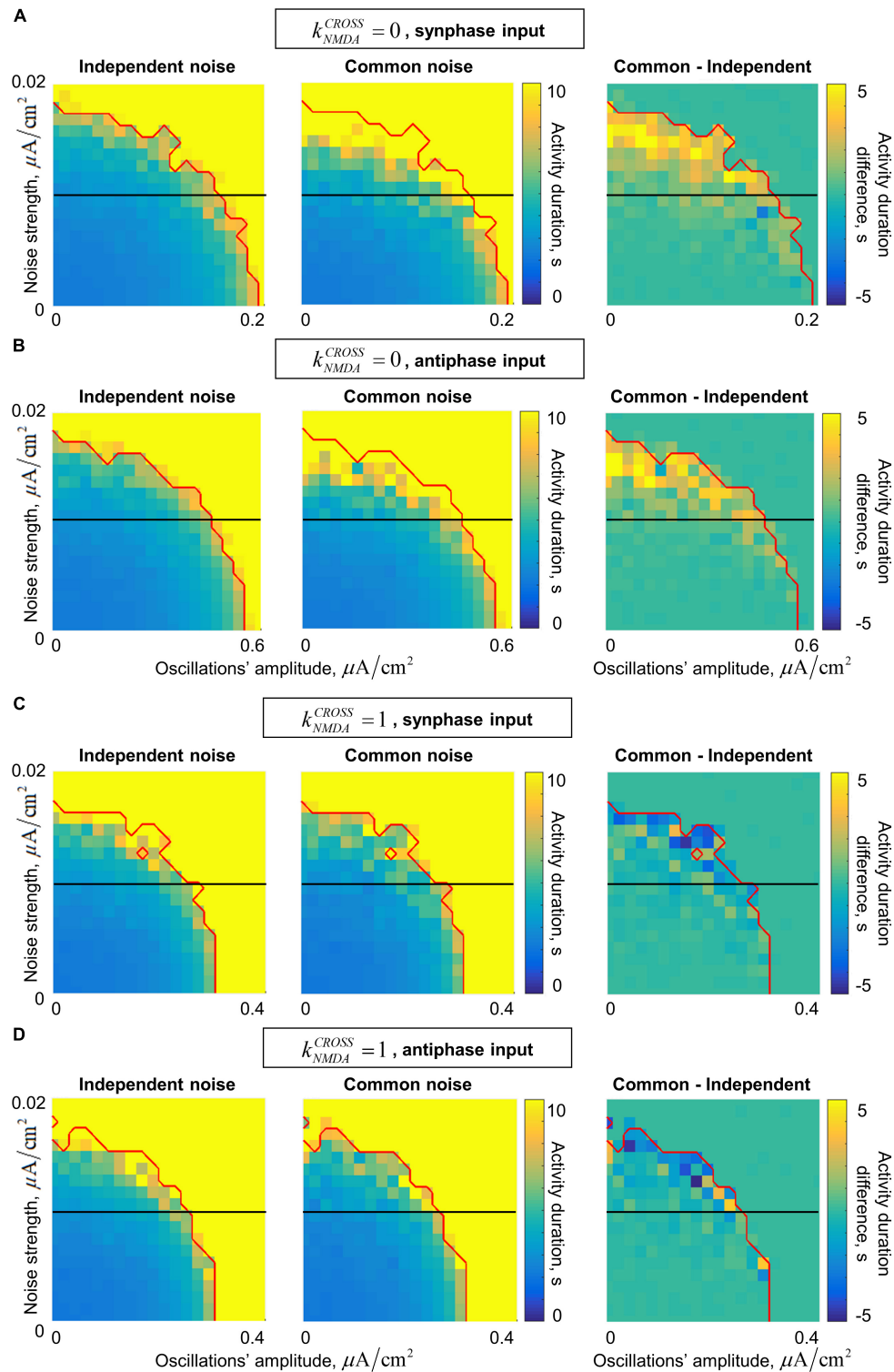


FIGURE 6 | Dependence of the post-stimulus activity duration in the two-circuit system on the amplitude of the input oscillations and the strength of the input noise for the in/anti-phase oscillations and two values of the NMDA connections strength. **(A,B)** Fast inter-circuit connection, **(C,D)** slow inter-circuit connections. **(A,C)** The circuits receive oscillatory signals in the same phase. **(B,D)** the circuits receive oscillatory signals in the opposite phases. Left column – each circuit receives an independent noise input; middle column – the circuits receive a common noise input; right column – the difference between these two cases. Red curve denotes the border of the saturation region: above this curve, the activity duration either for the common or for the independent noise case equals to the simulation time (i.e., above this curve comparison between the noise types does not make sense). Horizontal black lines denote the noise level of 0.01 (used further in the text). When the inter-circuit connections are fast, the activity is more robust (its duration is longer) in the case of common noise (yellow regions in the right panels of **(A,B)**). When the connections are slow, the activity is slightly more robust in the case of independent noise (blue regions in the right panels of **(C,D)**).

is the same). This is in contrast with the $k_{\text{NMDA}}^{\text{cross}} = 0$ case, in which in-phase input had much stronger effect than the anti-phase input. Such difference between $k_{\text{NMDA}}^{\text{cross}} = 0$ and $k_{\text{NMDA}}^{\text{cross}} = 1$ is in agreement with the result presented in **Figure 5** for a constant noise intensity. Let us, again, select a certain intermediate noise intensity (horizontal black lines in **Figures 6C,D**), and start to increase the gamma-band input amplitude. When the amplitude becomes high enough, the gamma-band input begins to stabilize the activity regime. This happens at slightly smaller amplitudes if the noise is independent, but irrespectively of whether the oscillatory input is in-phase or anti-phase.

Oscillatory Control of Multi-Circuit System

In this section, we show how the behavior of a multi-circuit system can be controlled by various types of oscillatory inputs. The results presented here are, in a large part, based on the effects of oscillations on two-circuit models described in the previous section. The multi-circuit system under consideration contains two clusters of circuits. Each cluster contains a group of circuits receiving a common noise input (the same signal for both clusters) and a group of circuits receiving independent noise inputs (we denote the “common-noise” groups of the first and second cluster as C1 and C2, respectively, and the “independent-noise” groups as I1 and I2). We consider two models – with fast and slow inter-cluster connections, respectively. We explore the behavior of the models in four conditions: (1) no oscillatory input (“NONE” condition), (2) only one cluster receives oscillatory input (“1CLUST” condition), (3) the clusters receive in-phase oscillations (“SYNC” condition), (4) the clusters receive anti-phase oscillations (“ANTI” condition). Each simulation was performed 25 times, and the statistics of group-averaged post-stimulus activity duration were collected for each of the four groups (C1, C2, I1, and I2) separately.

Figure 7 summarizes the results on the multi-circuit system behavior under the various oscillatory input conditions. The range of post-stimulus activity durations of the “common-noise” groups (C1 and C2) is represented by vertical red bars; the range of activity durations of the “independent-noise” groups (I1 and I2) – by vertical black bars. The horizontal dash in the middle of a bar marks the corresponding median value. Medians of the black and red bars obtained in the same condition are connected by black lines; a slope of such line demonstrates the difference in activity durations between the “common-noise” and “independent-noise” groups.

Without an oscillatory input (“NONE” condition), the groups receiving common noise input (C1 and C2) stay active for slightly longer time than the groups receiving independent noise inputs (I1 and I2). When the oscillatory input is delivered to the first cluster (“1CLUST” condition), it increases post-stimulus activity duration of both groups that belong to this cluster (C1 and I1). Importantly, the activity duration difference between the “common-noise” group (C1) and the “independent-noise” group (I1) also increases. These effects are almost absent for

the second cluster (groups C2 and I2) due to relatively weak inter-cluster interaction.

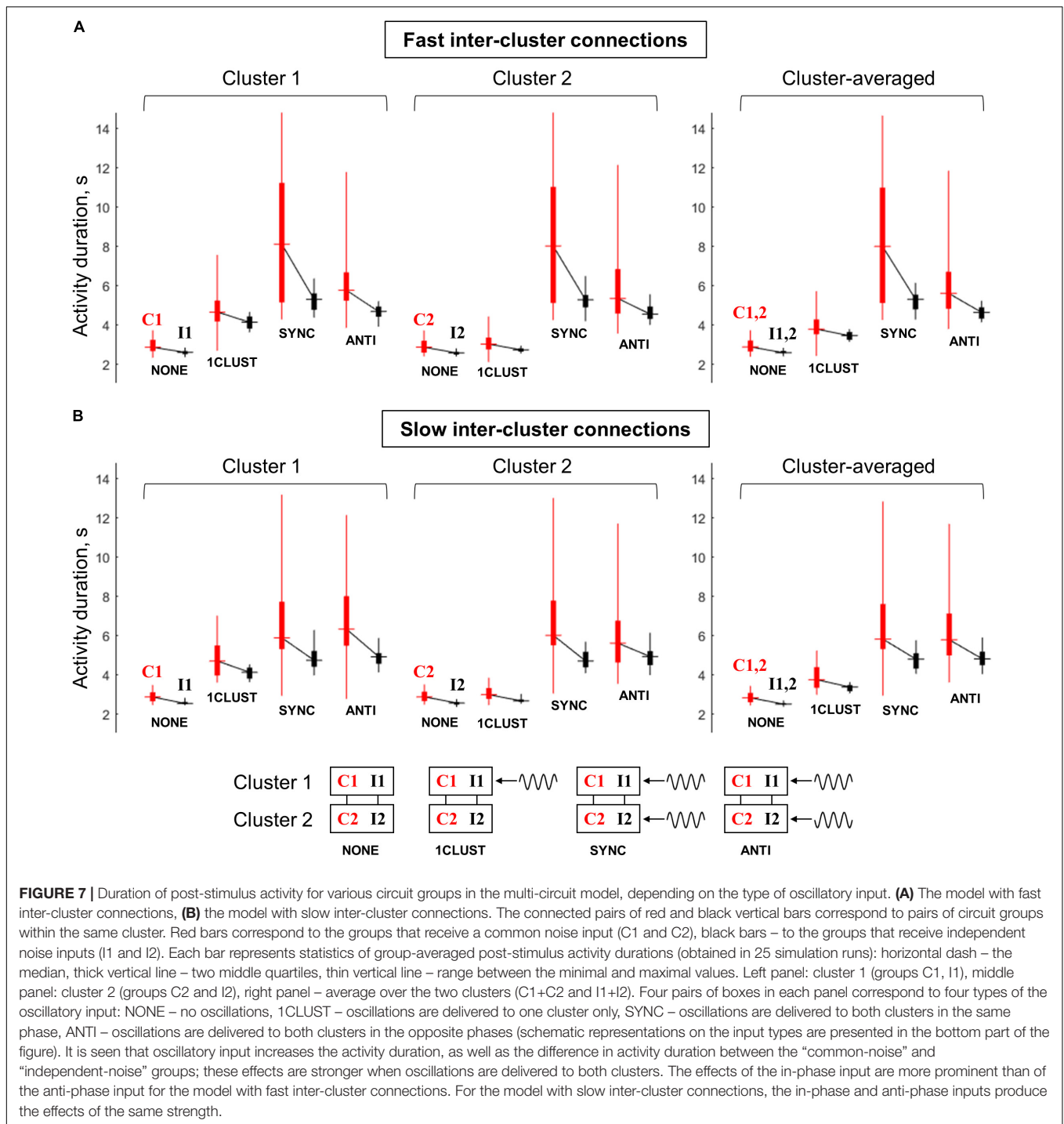
When the oscillations are delivered to both clusters, either in the same phase or in the antiphase (“SYNC” and “ANTI” conditions, respectively), they produce similar effects to one-cluster oscillatory input, but these effects are stronger and involve both clusters. Thus, post-stimulus activity duration for all the groups (C1, I1, C2, and I2), as well as activity duration difference between the “common-noise” and “independent-noise” groups (C1–I1 and C2–I2) are increased. In **Figure 7**, we can see that the activity duration is higher in “SYNC” and “ANTI” conditions, compared to “NONE” and “1CLUST” conditions for all noise input types (red and black), clusters (1 and 2) and model types (slow and fast inter-cluster connections). It is also seen that the links between the red and black boxes in both clusters (C1–I1 and C2–I2) are steeper in “SYNC”/“ANTI” conditions than in “NONE”/“1CLUST” conditions (for both model types), which reflects increased duration difference between the “common-noise” and “independent-noise” groups.

The models with fast and slow inter-cluster connections differ in their response to in-phase and anti-phase oscillatory inputs. In the model with fast connections, the in-phase input provides strong increase both in the activity duration and in the duration difference between the “common-noise” and “independent-noise” groups, while both these effects are considerably weaker in the case of the anti-phase input. On the contrary, in the model with slow inter-cluster connections, the in-phase and anti-phase oscillatory inputs lead to the effects of roughly the same strength. This difference between the two models is best visible in the results averaged over the clusters (right panels in **Figures 7A,B**). It is seen that the median levels and the slopes of the “red-black” links are higher for “SYNC” condition than for “ANTI” condition in the right panel of **Figure 7A**. At the same time, both the median levels and the slopes for “SYNC” and “ANTI” conditions are close to each other **Figure 7B**.

DISCUSSION

In this study, we considered several WM model variants, comprising of one, two, or many excitatory-inhibitory metastable circuits having mutual excitatory connections and receiving the same stimulus-related signal. First, we explored a single-circuit system and demonstrated that input gamma oscillations or white noise could stabilize (i.e., prolong) post-stimulus metastable activity. Next, we considered a two-circuit model and found that: (1) fast (AMPA) inter-circuit connections provide better stabilization by common-noise input compared to independent-noise inputs, (2) this difference could be further amplified by oscillatory inputs, (3) in-phase oscillatory inputs to the circuits produce better stabilization than anti-phase inputs in the case of fast (AMPA) connections, (4) in-phase and anti-phase inputs produce similar effects in the case of slow (NMDA) connections.

Finally, we developed a more realistic, multi-circuit system able to align with the effects observed in the two-circuit model. The system comprised of two clusters receiving in-phase or anti-phase oscillations and linked by fast (AMPA) or slow



(NMDA) connections. Each cluster contained a group of circuits that receive a common noise input (representing activity of a distributed WM representation this group is embedded in) and a group of circuits that receive independent inputs (and, thus, do not participate in the distributed WM retention). We found that: (1) oscillatory inputs stabilize activity of all circuits, (2) this stabilization is more pronounced for the “common-noise” groups compared to “independent-noise” groups, (3) in the case of fast

inter-cluster connections, both the stabilization and separation between the “common-noise” and “independent-noise” groups are more pronounced for in-phase input compared to anti-phase input, (4) in the case of slow connections, in-phase and anti-phase inputs produce comparable effects.

In summary, we demonstrated that gamma oscillations are able to selectively stabilize activity of the circuits that receive common noise input, thus supporting coherent activity of a

distributed WM representation. If long-range connections are fast, a part of this representation could be further highlighted by synchronizing gamma activity within this part. If these connections are slow, the distributed representation is uniformly stabilized, irrespective of phase differences between gamma oscillations in its local parts.

Single-Circuit System

We started from a single-circuit system and demonstrated that, with an appropriate parameter selection, both the noise and the gamma-band input alone could stabilize WM retention, without affecting the background regime. To explain these effects, we note that our model was tuned to operate in a subthreshold regime, in which the gain functions of the populations (excitatory and inhibitory) were concave. Consequently, even a zero-mean input (noisy or oscillatory) produced additional mean excitation to the populations. In our system, the mean effect of oscillations on the excitatory population outweighed their effect on the inhibitory population, which resulted in oscillation-induced/noise-induced mean firing rate increase and, consequently, to stabilization of the active regime.

A similar effect – stabilization of initially metastable active regime in a WM model by gamma-band input – was previously demonstrated by Schmidt et al. (2018). In this study, the authors considered a purely excitatory system, but took into account the effect of spike-to-spike synchronization, which allowed to achieve resonant behavior without inhibitory population. The system had a resonance in the beta band, but the stabilization occurred under high-gamma input, while beta-band input, on the contrary, switched the system to the background state. A similar switching to the background state by a resonant input was also reported by Dipoppa and Gutkin (2013). In our model, we do not observe this effect, presumably due to the presence of slow NMDA currents and short-term plasticity, which make the activity more robust to transient episodes of synchronization. As a result, the effect of input oscillations is always excitatory in our model.

We should note that our model is more biologically realistic, compared to Dipoppa and Gutkin (2013) and Schmidt et al. (2018). First, it contains both an excitatory and an inhibitory population. Second, it operates in a subthreshold regime [which is typical for cortical networks during WM retention, (Compte et al., 2003)], while in the aforementioned models, the neurons operated mostly in a suprathreshold regime with regular spiking activity. Third, both these models used highly non-linear pulse-like periodic inputs, while in our case, the oscillatory input was sinusoidal [which is, again, closer to the situation in the neocortex; (see Wang, 2010)].

Two-Circuit System

In the two-circuit system, under a constant noise intensity, we demonstrated that in-phase gamma-band input stabilizes WM retention much more effectively than anti-phase input when inter-circuit interaction is fully mediated by fast AMPA receptors ($k_{\text{NMDA}}^{\text{cross}} = 0$). With increasing NMDA:AMPA ratio of the inter-circuit connections, effectiveness of the in-phase gamma-band input decreased, while effectiveness of the anti-phase input increased. When the interaction was fully mediated by slow

NMDA receptors ($k_{\text{NMDA}}^{\text{cross}} = 1$), effectiveness of in-phase and anti-phase input was about the same.

The observed effects could be explained by the fact that the eigenmode of the system is in-phase if $k_{\text{NMDA}}^{\text{cross}} = 0$ and anti-phase if $k_{\text{NMDA}}^{\text{cross}} = 1$. This fact is illustrated in **Supplementary Figures 2E, 3E**. Without oscillatory input, independent noise inputs lead to in-phase quasi-oscillations if $k_{\text{NMDA}}^{\text{cross}} = 0$ (left part of **Supplementary Figure 2E**, black curve); however, if $k_{\text{NMDA}}^{\text{cross}} = 1$, then the noise-induced quasi-oscillations have the average phase difference between the circuits closer to π (left part of **Supplementary Figure 3E**, black curve). The most effective entrainment (and, thus, the most effective stabilization) occurs when the phase difference between the inputs to the circuits matches the eigenmode of the system. In the case of $k_{\text{NMDA}}^{\text{cross}} = 0$, anti-phase input should change activity of the system from the in-phase to the anti-phase mode to fully entrain it (**Supplementary Figure 2F**), which is accompanied by oscillation-induced desynchronization at certain input amplitudes (**Supplementary Figure 2D**); in the case of $k_{\text{NMDA}}^{\text{cross}} = 1$, the anti-phase entrainment is much easier (**Supplementary Figures 3D,F**). On the contrary, in-phase oscillations more easily entrain the system if $k_{\text{NMDA}}^{\text{cross}} = 0$ (**Supplementary Figures 2C,E**), rather than if $k_{\text{NMDA}}^{\text{cross}} = 1$ (**Supplementary Figures 3C,E**).

We next considered how the duration of post-stimulus activity (i.e., effectiveness of the active regime stabilization) jointly depends on noise intensity and gamma-band input amplitude. For the fast inter-circuit connections ($k_{\text{NMDA}}^{\text{cross}} = 0$), common noise stabilized the active regime more effectively than independent noise. On the contrary, for the slow inter-circuit connections ($k_{\text{NMDA}}^{\text{cross}} = 1$), independent noise was slightly more effective. Importantly, for intermediate noise intensities, there was a range of gamma amplitudes, in which the gamma-band input stabilized the active regime with considerably different effectiveness depending on the noise type (common / independent). We used this effect as the basis for selective oscillatory control of activity robustness in the multi-circuit system.

The higher effectiveness of the common noise in the case of $k_{\text{NMDA}}^{\text{cross}} = 0$ could be, again, explained by the fact that the system's eigenmode in this case is in-phase. Common noise fully projects to this mode, while independent noise projects to it only partially. Thus, entrainment of the in-phase mode by independent noise is weaker, which leads to smaller stabilizing effect. On the contrary, independent noise partially projects to the anti-phase mode (which is the eigenmode of the system with $k_{\text{NMDA}}^{\text{cross}} = 1$), while common noise is orthogonal to this mode, so independent noise is more effective when $k_{\text{NMDA}}^{\text{cross}} = 1$.

There is another effect that possibly participates in the link between $k_{\text{NMDA}}^{\text{cross}}$ and activity robustness. Since slow NMDA receptors provide low-pass filtering of activity, they make the system less resonant. Consequently, increase of $k_{\text{NMDA}}^{\text{cross}}$ decreases the amplitude of entrained oscillations or noise-induced quasi-oscillations (compare left parts of **Supplementary Figures 2G, 3G**). This effect presumably sums up with the aforementioned effects of eigenmode matching by external inputs.

We note that worsening of the stabilization by in-phase oscillations for higher NMDA:AMPA ratio seemingly contradicts earlier results suggesting the stabilizing role of NMDA receptors in WM retention in the presence of oscillatory activity (Tegnér et al., 2002). This discrepancy could be explained by the fact that the model used in Tegnér et al. (2002) is bistable, but does not contain any slow variables except of the NMDA current. Consequently, the system in the active state is stable in the absence of fluctuations, but fast fluctuations (such as gamma oscillations) make it fall down to the background state if the NMDA:AMPA ratio is too small. On the contrary, our model is metastable, so it spontaneously returns from the active regime to the background state in the absence of fluctuations. At the same time, our system contains slow variables besides the inter-circuit NMDA current – namely, within-circuit NMDA currents and coefficients of within-circuit short-term plasticity. As the result, our system is resistant to fast fluctuations (i.e., it survives fluctuation-induced “gaps” in the activity), even if the within-circuit NMDA:AMPA ratio is zero. Fast fluctuations, instead, increase the level of activity (thus stabilizing it) due to concavity of the gain functions. Notably, the ability of periodic input to stabilize metastable regime even in a model without slow variables was previously demonstrated by Schmidt et al. (2018). We suggest that the stabilizing effect of NMDA current described in Tegnér et al. (2002) could be also present in our model, but it is weak compared to the other effects we described.

Multi-Circuit System

In the analysis of the two-circuit system, we observed two important effects. First, in the case of fast connections and intermediate noise level, input oscillations could strongly stabilize WM retention in a pair of circuits receiving a common noise input, while producing much weaker effect on circuits receiving independent noise inputs. Second, if the connections between two circuits are fast, then the stabilizing effect of oscillations is considerably stronger when oscillations are delivered to the circuits in the same phase rather than in the opposite phases; however, this difference is mitigated if the inter-circuit connections are slow.

In order to demonstrate how these effects could be scaled up and utilized for oscillatory control of WM retention, we developed a multi-circuit system. We assumed that WM retention is based on distributed neural activity, and that local cortical patches could contain circuits involved in this activity, as well as circuits not involved in it (a similar scheme was used in Lundqvist et al. (2011), in which local modules contained parts of various representations, and corresponding parts in different modules were connected by long-range projections). We explicitly included two local patches (referred to as clusters) into our WM system and modeled the inputs from other parts of the cortex as white-noise signals. The circuits in each cluster formed two groups, named C1, I1 in the first cluster, and C2, I2 – in the second one. The groups C1, C2 were considered to participate in the coherent distributed activity related to WM retention, so the circuits from these groups received common noise input. The groups I1, I2 did not participate in this activity, so their circuits received independent noise inputs. We note that,

unlike most WM models (e.g., Brunel and Wang, 2001; Lundqvist et al., 2011), participation of a group in the WM representation is not determined at the stimulus presentation stage, since all the circuits in our model receive the same stimulus signal. Instead, a group is considered to be a part of the WM representation if its circuits receive common noise input.

We demonstrated that, as in the two-circuit case, gamma-band input can stabilize WM retention, i.e., increase post-stimulus activity duration. Importantly, this stabilization was more prominent for the “common-noise” groups (C1 and C2), compared to the “independent-noise” groups (I1 and I2). Thus, the gamma-band input also increased “selectivity” of WM retention, predominantly stabilizing those circuits that participate in WM-related distributed coherent activity. This behavior is in agreement with the reported increase in both the firing rates and stimulus selectivity that occurs on top of elevated gamma activity episodes during WM retention (Lundqvist et al., 2016, 2018; Bastos et al., 2018). Such functionality of gamma-input in our model is achieved due to high AMPA-based within-group connectivity and low inter-group connectivity. As a consequence of this, circuit pairs with common noise input and pairs with independent inputs are mostly separated from each other, so the results obtained for the two-circuit system are still applicable. If the inter-group connections are too dense, correlations would spread across the whole system, and the difference between the “common-noise” and “independent-noise” circuits would be diminished.

We suggest that the dense within-group and sparse inter-group connectivity follows naturally from the Hebbian plasticity principles: the circuits that receive the same input (members of C1 and C2) would instantiate links between each other. We assume that the “independent-input” circuits (members of I1 and I2) could also participate in the dominant active representation (and thus receive a common input) in certain cases that we do not model explicitly here: e.g., for different WM content or different task rules. On the contrary, since the groups C1 and I1 (as well as C2 and I2) participate in different representations, their circuits do not usually receive common inputs, which justifies sparse inter-group (C1–I1 and C2–I2) connections.

We also confirmed in the multi-circuit module the influence of NMDA:AMPA ratio on the system’s tendency to respond differently depending on the phase between gamma-band oscillatory inputs delivered to its parts. We demonstrated that the stabilizing effect of the input oscillations (i.e., oscillation-induced prolongation of post-stimulus activity) in the system with fast (AMPA-based) inter-cluster connections is stronger when the oscillations are delivered to the clusters in the same phase rather than in the opposite phases. On the contrary, the stabilizing effect of the in-phase and anti-phase inputs to the clusters was the same in the case of slow (NMDA-based) inter-cluster connections. This difference between the slow and fast inter-cluster connections was observed only when the connectivity between the corresponding groups of different clusters (C1–C2 and I1–I2) was weaker than the within-group connectivity. We suggest that such layout is biologically plausible, due to presumed small-world character of the cortical topology

(Bullmore and Sporns, 2009; Bassett and Bullmore, 2017), with long-range connections being, in general, sparser than short-range connections (Ercsey-Ravasz et al., 2013).

Thus, fast and slow inter-cluster connections provide different functionality. Fast connections allow to selectively increase retention robustness in a part of an active distributed representation by synchronizing it in the gamma-band (e.g., by providing common gamma-band input from a controller cortical or subcortical network). In turn, slow inter-cluster connections provide a basis for robust WM retention by a distributed network with local gamma generators, which do not need to be synchronized. We note that the local character of gamma oscillations is experimentally supported (Donner and Siegel, 2011), and it was also assumed in previous multi-modular models of WM (Lundqvist et al., 2011).

DATA AVAILABILITY STATEMENT

The original contributions presented in the study are included in the article/**Supplementary Material**, further inquiries can be directed to the corresponding author/s.

REFERENCES

- Amit, D. J., and Brunel, N. (1997). Model of global spontaneous activity and local structured activity during delay periods in the cerebral cortex. *Cereb. Cortex* 7, 237–252. doi: 10.1093/cercor/7.3.237
- Ardid, S., Wang, X. J., Gomez-Cabrero, D., and Compte, A. (2010). Reconciling coherent oscillation with modulation of irregular spiking activity in selective attention: gamma-range synchronization between sensory and executive cortical areas. *J. Neurosci.* 30, 2856–2870. doi: 10.1523/JNEUROSCI.4222-09.2010
- Augustin, M., Ladenbauer, J., Baumann, F., and Obermayer, K. (2017). Low-dimensional spike rate models derived from networks of adaptive integrate-and-fire neurons: comparison and implementation. *PLoS Comput. Biol.* 13:e1005545. doi: 10.1371/journal.pcbi.1005545
- Baddeley, A. (2003). Working memory: looking back and looking forward. *Nat. Rev. Neurosci.* 4, 829–839. doi: 10.1038/nrn1201
- Bassett, D. S., and Bullmore, E. T. (2017). Small-world brain networks revisited. *Neuroscientist* 23, 499–516. doi: 10.1177/1073858416667720
- Bastos, A. M., Loonis, R., Kornblith, S., Lundqvist, M., and Miller, E. K. (2018). Laminar recordings in frontal cortex suggest distinct layers for maintenance and control of working memory. *Proc. Natl. Acad. Sci. U.S.A.* 115, 1117–1122. doi: 10.1073/pnas.1710323115
- Brunel, N., and Wang, X. J. (2001). Effects of neuromodulation in a cortical network model of object working memory dominated by recurrent inhibition. *J. Comput. Neurosci.* 11, 63–85. doi: 10.1023/a:1011204814320
- Bullmore, E., and Sporns, O. (2009). Complex brain networks: graph theoretical analysis of structural and functional systems. *Nat. Rev. Neurosci.* 10, 186–198. doi: 10.1038/nrn2575
- Chafee, M. V., and Goldman-Rakic, P. S. (1998). Matching patterns of activity in primate prefrontal area 8a and parietal area 7ip neurons during a spatial working memory task. *J. Neurophysiol.* 79, 2919–2940. doi: 10.1152/jn.1998.79.6.2919
- Chik, D. (2013). Theta-alpha cross-frequency synchronization facilitates working memory control – a modeling study. *Springerplus* 2:14. doi: 10.1186/2193-1801-2-14
- Compte, A. (2006). Computational and in vitro studies of persistent activity: edging towards cellular and synaptic mechanisms of working memory. *Neuroscience* 139, 135–151. doi: 10.1016/j.neuroscience.2005.06.011
- Compte, A., Constantinidis, C., Tegnér, J., Raghavachari, S., Chafee, M. V., Goldman-Rakic, P. S., et al. (2003). Temporally irregular

AUTHOR CONTRIBUTIONS

NN carried out the research. NN, DZ, and BG conceived the research. NN, DZ, VM, and BG discussed the results and wrote the manuscript. All authors contributed to the article and approved the submitted version.

FUNDING

This article is an output of a research project implemented as part of the Basic Research Program at the National Research University Higher School of Economics (HSE University). BG acknowledges support from CNRS, INSERM, ANR-17-EURE-0017, and ANR-10-IDEX-0001-02.

SUPPLEMENTARY MATERIAL

The Supplementary Material for this article can be found online at: <https://www.frontiersin.org/articles/10.3389/fncir.2021.647944/full#supplementary-material>

- mnemonic persistent activity in prefrontal neurons of monkeys during a delayed response task. *J. Neurophysiol.* 90, 3441–3454. doi: 10.1152/jn.0949.2002
- Constantinidis, C., and Goldman-Rakic, P. S. (2002). Correlated discharges among putative pyramidal neurons and interneurons in the primate prefrontal cortex. *J. Neurophysiol.* 88, 3487–3497. doi: 10.1152/jn.00188.2002
- Dipoppa, M., and Gutkin, B. S. (2013). Flexible frequency control of cortical oscillations enables computations required for working memory. *Proc. Natl. Acad. Sci. U.S.A.* 110, 12828–12833. doi: 10.1073/pnas.1303270110
- Donner, T. H., and Siegel, M. (2011). A framework for local cortical oscillation patterns. *Trends Cogn. Sci.* 15, 191–199. doi: 10.1016/j.tics.2011.03.007
- Ercsey-Ravasz, M., Markov, N. T., Lamy, C., Van Essen, D. C., Knoblauch, K., Toroczka, Z., et al. (2013). A predictive network model of cerebral cortical connectivity based on a distance rule. *Neuron* 80, 184–197. doi: 10.1016/j.neuron.2013.07.036
- Funahashi, S., Bruce, C. J., and Goldman-Rakic, P. S. (1989). Mnemonic coding of visual space in the monkey's dorsolateral prefrontal cortex. *J. Neurophysiol.* 61, 331–349. doi: 10.1152/jn.1989.61.2.331
- Fuster, J. M., and Alexander, G. E. (1971). Neuron activity related to short-term memory. *Science* 173, 652–654.
- Goldman-Rakic, P. S. (1995). Cellular basis of working memory. *Neuron* 14, 477–485.
- Gutkin, B. S., Laing, C. R., Colby, C. L., Chow, C. C., and Ermentrout, G. B. (2001). Turning on and off with excitation: the role of spike-timing asynchrony and synchrony in sustained neural activity. *J. Comput. Neurosci.* 11, 121–134. doi: 10.1023/A:1012837415096
- Haegens, S., Osipova, D., Oostenveld, R., and Jensen, O. (2010). Somatosensory working memory performance in humans depends on both engagement and disengagement of regions in a distributed network. *Hum. Brain Mapp.* 31, 26–35. doi: 10.1002/hbm.20842
- Hansel, D., and Mato, G. (2013). Short-term plasticity explains irregular persistent activity in working memory tasks. *J. Neurosci.* 33, 133–149. doi: 10.1523/JNEUROSCI.3455-12.2013
- Howard, M. W., Rizzuto, D. S., Caplan, J. B., Madsen, J. R., Lisman, J., Aschenbrenner-Scheibe, R., et al. (2003). Gamma oscillations correlate with working memory load in humans. *Cereb Cortex* 13, 1369–1374. doi: 10.1093/cercor/bhg084
- Jokisch, D., and Jensen, O. (2007). Modulation of gamma and alpha activity during a working memory task engaging the dorsal or ventral stream. *J. Neurosci.* 27, 3244–3251. doi: 10.1523/JNEUROSCI.5399-06.2007

- Kaiser, J., Ripper, B., Birbaumer, N., and Lutzenberger, W. (2003). Dynamics of gamma-band activity in human magnetoencephalogram during auditory pattern working memory. *Neuroimage* 20, 816–827. doi: 10.1016/S1053-8119(03)00350-1
- Kopell, N., Whittington, M. A., and Kramer, M. A. (2011). Neuronal assembly dynamics in the beta frequency range permits short-term memory. *Proc. Natl. Acad. Sci. U.S.A.* 108, 3779–3784. doi: 10.1073/pnas.1019676108
- Kornblith, S., Buschman, T. J., and Miller, E. K. (2016). Stimulus load and oscillatory activity in higher cortex. *Cereb. Cortex* 26, 3772–3784. doi: 10.1093/cercor/bhv182
- Laing, C. R., and Chow, C. C. (2001). Stationary bumps in networks of spiking neurons. *Neural Comput.* 13, 1473–1494. doi: 10.1162/089976601750264974
- Liebe, S., Hoerzer, G. M., Logothetis, N. K., and Rainer, G. (2012). Theta coupling between V4 and prefrontal cortex predicts visual short-term memory performance. *Nat. Neurosci.* 15, 456–462. doi: 10.1038/nn.3038
- Lim, S., and Goldman, M. S. (2013). Balanced cortical microcircuitry for maintaining information in working memory. *Nat. Neurosci.* 16, 1306–1314. doi: 10.1038/nn.3492
- Lisman, J. E., and Idiart, M. A. P. (1995). Storage of 7 ± 2 short-term memories in oscillatory subcycles. *Science* 267, 1512–1515. doi: 10.1126/science.7878473
- Lundqvist, M., Compte, A., and Lansner, A. (2010). Bistable, irregular firing and population oscillations in a modular attractor memory network. *PLoS Comput. Biol.* 6:e1000803. doi: 10.1371/journal.pcbi.1000803
- Lundqvist, M., Herman, P., and Lansner, A. (2011). Theta and gamma power increases and alpha/beta power decreases with memory load in an attractor network model. *J. Cogn. Neurosci.* 23, 3008–3020. doi: 10.1162/jocn_a.00029
- Lundqvist, M., Herman, P., Warden, M. R., Brincat, S. L., and Miller, E. K. (2018). Gamma and beta bursts during working memory readout suggest roles in its volitional control. *Nat. Commun.* 9:394. doi: 10.1038/s41467-017-02791-8
- Lundqvist, M., Rose, J., Herman, P., Brincat, S. L., Buschman, T. J., and Miller, E. K. (2016). Gamma and beta bursts underlie working memory. *Neuron* 90, 152–164. doi: 10.1016/j.neuron.2016.02.028
- Lutzenberger, W., Ripper, B., Busse, L., Birbaumer, N., and Kaiser, J. (2002). Dynamics of gamma-band activity during an audiospatial working memory task in humans. *J. Neurosci.* 22, 5630–5638. doi: 10.1523/JNEUROSCI.22-13-05630.2002
- Miller, E. K., Erickson, C. A., and Desimone, R. (1996). Neural mechanisms of visual working memory in prefrontal cortex of the macaque. *J. Neurosci.* 16, 5154–5167. doi: 10.1523/JNEUROSCI.16-16-05154.1996
- Mongillo, G., Barak, O., and Tsodyks, M. (2008). Synaptic theory of working memory. *Science* 319, 1543–1546. doi: 10.1126/science.1150769
- Mongillo, G., Hansel, D., and van Vreeswijk, C. (2012). Bistability and spatio-temporal irregularity in neuronal networks with nonlinear synaptic transmission. *Phys. Rev. Lett.* 108:158101. doi: 10.1103/PhysRevLett.108.158101
- Palva, J. M., Monto, S., Kulashekhar, S., and Palva, S. (2010). Neuronal synchrony reveals working memory networks and predicts individual memory capacity. *Proc. Natl. Acad. Sci. U.S.A.* 107, 7580–7585. doi: 10.1073/pnas.0913113107
- Palva, S., Kulashekhar, S., Hämäläinen, M., and Palva, J. M. (2011). Localization of cortical phase and amplitude dynamics during visual working memory encoding and retention. *J. Neurosci.* 31, 5013–5025. doi: 10.1523/JNEUROSCI.5592-10.2011
- Pina, J. E., Bodner, M., and Ermentrout, B. (2018). Oscillations in working memory and neural binding: a mechanism for multiple memories and their interactions. *PLoS Comput. Biol.* 14:e1006517. doi: 10.1371/journal.pcbi.1006517
- Renart, A., Moreno-Bote, R., Wang, X. J., and Parga, N. (2007). Mean-driven and fluctuation-driven persistent activity in recurrent networks. *Neural Comput.* 19, 1–46. doi: 10.1162/neco.2007.19.1.1
- Roux, F., and Uhlhaas, P. J. (2014). Working memory and neural oscillations: α - γ versus θ - γ codes for distinct WM information? *Trends Cogn. Sci.* 18, 16–25. doi: 10.1016/j.tics.2013.10.010
- Roxin, A., and Compte, A. (2016). Oscillations in the bistable regime of neuronal networks. *Phys. Rev. E* 94:012410. doi: 10.1103/PhysRevE.94.012410
- Sauseng, P., Klimesch, W., Heise, K. F., Gruber, W. R., Holz, E., Karim, A. A., et al. (2009). Brain oscillatory substrates of visual short-term memory capacity. *Curr. Biol.* 19, 1846–1852. doi: 10.1016/j.cub.2009.08.062
- Schaffer, E. S., Ostojic, S., and Abbott, L. F. (2013). A complex-valued firing-rate model that approximates the dynamics of spiking networks. *PLoS Comput. Biol.* 9:e1003301. doi: 10.1371/journal.pcbi.1003301
- Schmidt, H., Avitabile, D., Montbrió, E., and Roxin, A. (2018). Network mechanisms underlying the role of oscillations in cognitive tasks. *PLoS Comput. Biol.* 14:e1006430. doi: 10.1371/journal.pcbi.1006430
- Sherfey, J., Ardid, S., Miller, E. K., Hasselmo, M. E., and Kopell, N. J. (2020). Prefrontal oscillations modulate the propagation of neuronal activity required for working memory. *Neurobiol. Learn. Mem.* 173:107228. doi: 10.1016/j.nlm.2020.107228
- Siegel, M., Warden, M. R., and Miller, E. K. (2009). Phase-dependent neuronal coding of objects in short-term memory. *Proc. Natl. Acad. Sci. U.S.A.* 106, 21341–21346. doi: 10.1073/pnas.0908193106
- Tegnér, J., Compte, A., and Wang, X. J. (2002). The dynamical stability of reverberatory neural circuits. *Biol. Cybern.* 87, 471–481. doi: 10.1007/s00422-002-0363-9
- Tseng, P., Chang, Y.-T., Chang, C.-F., Liang, W.-K., and Juan, C.-H. (2016). The critical role of phase difference in gamma oscillation within the temporoparietal network for binding visual working memory. *Sci. Rep.* 6:32138. doi: 10.1038/srep32138
- Tsodyks, M. V., and Markram, H. (1997). The neural code between neocortical pyramidal neurons depends on neurotransmitter release probability. *Proc. Natl. Acad. Sci. U.S.A.* 94, 719–723. doi: 10.1073/pnas.94.2.719
- van Vugt, M. K., Schulze-Bonhage, A., Litt, B., Brandt, A., and Kahana, M. J. (2010). Hippocampal gamma oscillations increase with memory load. *J. Neurosci.* 30, 2694–2699. doi: 10.1523/JNEUROSCI.0567-09.2010
- Wang, X. J. (2001). Synaptic reverberation underlying mnemonic persistent activity. *Trends Neurosci.* 24, 455–463. doi: 10.1016/s0166-2236(00)01868-3
- Wang, X. J. (2010). Neurophysiological and computational principles of cortical rhythms in cognition. *Physiol. Rev.* 90, 1195–1268. doi: 10.1152/physrev.00035.2008
- Wimmer, K., Ramon, M., Pasternak, T., and Compte, A. (2016). Transitions between multiband oscillatory patterns characterize memory-guided perceptual decisions in prefrontal circuits. *J. Neurosci.* 36, 489–505. doi: 10.1523/JNEUROSCI.3678-15.2016

Conflict of Interest: The authors declare that the research was conducted in the absence of any commercial or financial relationships that could be construed as a potential conflict of interest.

Copyright © 2021 Novikov, Zakharov, Moiseeva and Gutkin. This is an open-access article distributed under the terms of the Creative Commons Attribution License (CC BY). The use, distribution or reproduction in other forums is permitted, provided the original author(s) and the copyright owner(s) are credited and that the original publication in this journal is cited, in accordance with accepted academic practice. No use, distribution or reproduction is permitted which does not comply with these terms.